Journal of Fluorescence (2025) 35:8959–8972
https://doi.org/10.1007/s10895-025-04152-x

RESEARCH

Selective Identification and Quantification of Microplastics Using Solid Fluorescent Green Carbon Dots (SFGCDs) – A Novel, Naked Eye Sensing Fluoroprobe

Ayun R. Jini[1] · G. Gnanamani Simiyon[1] · T. Mary Vergheese[1]

Received: 24 November 2024 / Accepted: 22 January 2025 / Published online: 27 February 2025

Abstract

The current work presents a Novel, Carbon Dot fluoroprobe to selectively identify and quantify Microplastics (MPs) released from Surgical facemask and Cosmetic Personal Cleansers. Solid Fluorescent Green Carbon Dots (SFGCDs) are synthesized for the first time from a high carbon source natural resin, obtained from *Araucaria araucana* (Monkey puzzle tree). The increased carbon content is responsible for the green colour of the CDs. SFGCDs function as a TURN OFF fluoroprobe on detection of MPs through dynamic quenching mechanism, which is confirmed from Stern Volmer Plot with an R^2 value of. The minimum LOD being 0.0063 g/l for ≥ 6 µm diameter MPs. The agglomeration of microplastics released from surgical mask and cosmetic cleansers on functions as an insulator on the surface of SFGCDs, forbidding ease of electron- hole transfer between the donor- SFGCDs and acceptor-MPs. The release of MPs from the donor surface results in reappearance of fluorescence obeying FRET mechanism. The detection of MPs/ microfibres released by disposable surgical mask is studied by the degradation of the surgical face mask for a period of 50 days, followed by detection. Turn- OFF in fluorescence of SFGCDs observed in presence of micro fibre Turns On, as remediation of MPs is done by a simple filtration technique. The results demonstrate the potential of the fluoroprobe towards real time detection of MPs and simple remediation of MPs to conserve the ecosystem. The SFGCDs is stable and can be reused for nearly 3 cycles for the detection of MPs. A single PL peak obtained on detection of MPs in presence of monovalent, divalent trivalent ions and biomolecules authenticates the selectivity and stability of SFGCDs to function as an efficient fluoroprobe towards sensing of MPs.

Graphical Abstract

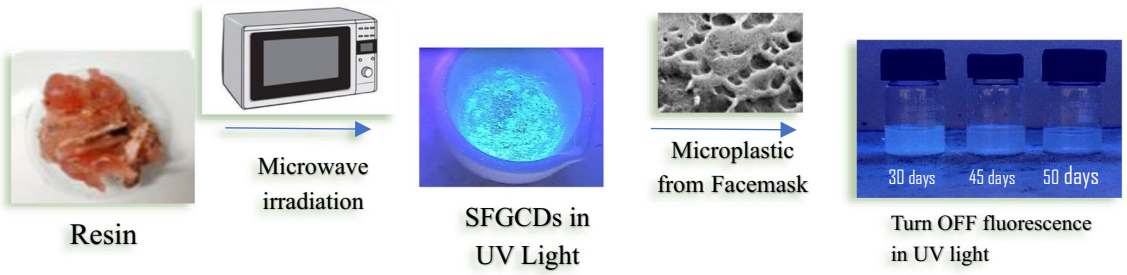

Keywords Green carbon dots · FRET · Microplastics · Fluoroprobe · Dynamic quenching

Introduction

UN goal 14 mentions to conserve and sustainably use the oceans, seas and marine resources responsibly where in the target by 2025 is to prevent and significantly reduce pollution of all kinds in particular plastic debris. Plastics,

✉ T. Mary Vergheese
maryvergheese@mcc.edu.in

[1] Department of Chemistry, Madras Christian College, Chennai 600059, Tamil Nadu, India

the non- biodegradable pollutant only disintegrates in the environment as mega plastics (length > 50 cm), macro plastics (length > 5 to 50 cm), meso plastics (length 5 mm to 5 cm), microplastics (length 1 mm to 5 mm), nano plastics (length < 1 mm) [1]. Research shows a longer shelf life of Microplastics (MPs) and the percentage of pollution due to MPs in water is the highest compared to air and land [2–5]. One type of substance that may readily enter a person's body through food chains is MPs [6].Thus, MPs affects the health of every organism i.e. Increases the algal growth in marine system, suffocates breathing of soil and humans and finally MPs becomes a menace to the ecosystem. Microplastics are polymers like Polyethylene (PE), Polypropylene(PP), polyvinyl chloride (PVC), polystyrene (PS), polyamide (PA) and PET [7, 8]. Microscale grains or debris of plastics according to the US National Oceanic and Atmospheric Administration (NOAA) are classified as primary and secondary MPs [9]. When bigger raw plastic particles are exposed to chemical and physical variables such as weathering, pressure, and UV light, secondary MPs are formed [10–12]. The identification of MPs in the environment becomes very tedious because UV radiation, oxidation and mechanical forces break MPs to fragments smaller than 5 µm in diameter.

During and post COVID-19 pandemic the use of disposable surgical mask has become an inevitable part of our daily life. Once after use, they are carelessly thrown off into the ecosystem without obeying proper disposal procedures. These disposed masks degrade in environment to release MPs in the form of fibres, reach the water stream and continues degrading. As its size is very small, colourless, it remains unnoticed to naked eye, and hence becomes a concern to the inhabitants in the environment [13]. Earlier studies revealed surgical masks shed more than 100 to 200 microfibers over a week, identifying these fibres as polypropylene [14].The other sources of MPs are industries such as textiles, pharmaceuticals and cosmetics which utilize MPs for various applications [15]. MPs, a ubiquitous environmental pollutant sought widespread attention after reports about its pollution caused to human health [16, 17], marine life [14], and agricultural pollutants [18] were brought to attention by researchers. The health of habitats in land and water becomes a concern due to build-up of MPs of varying sizes and types enter their food chain making detection and remediation of MPs inevitable to protect the earth and preserve the BLUE.

Earlier studies have reported the detection of MPs by CeO_2 NPs using Electrochemical method [19], Surface nanodroplet by Microfluidic detection using Raman Spectroscopy [20], by Au NPs using SERS detection [21], by Au NPs thin film using SERS [22], by Ag NPs using SERS [23], by Au NPs using Colorimetric method [24]. Fourier transform infrared spectroscopy (FTIR) [25], scanning electron microscopy–energy-dispersive X-ray (SEM–EDX) [26], thermal analysis [27] and Raman spectroscopy [28] are a few techniques reported to detect MPs. The above-mentioned techniques are not economical and at the same time the precursors used are also not easy to synthesize and commercialize. Detection of MPs by Carbon Dots (CDs) is not yet reported, similarly the Photoluminescence technique to detect MPs using CDs as the nanoprobe is also not yet been reported. CDs are non -toxic, ecofriendly and easy to synthesize. Hence, this current work reports the detection of MPs by naked eye using nontoxic, economical, ecofriendly nanoprobe CDs synthesised from green source by means of a simple fluorescence technique.

Cosmetic products contain coloured and colourless MPs and the detection of the same is very difficult when it reaches the water stream. Similarly, disposable masks when reaches water stream gets degraded to [29] extremely small, fibre-shaped microplastics which are more dangerous to nature. Thus, the current work aims in detection of MPs released from cosmetic cleanser and disposable face mask.

Carbon dots (CDs), fluorescent carbon-based nanomaterial with a size of less than 10 nm is gaining popularity in recent years [30, 31]. These carbon-based nanomaterials have sp^2 /sp^3 skeletons with ample functional groups such as carboxyl, hydroxyl, amine, etc. with a graphite lattice or amorphous carbon form [32]. The covalent character of the carbon skeleton structure enhances CDs stability and functions as a potential tool for various application. CDs are reported to be non-toxic and highly biocompatible. Fluorescence is one of the important characteristic features of CDs where the electron–hole pair recombination occurs in minuscule sp^2 carbon clusters embedded in the sp^3 matrix [33, 34] Fluorescent quenching, change in colour of the fluorescence or increase in intensity of fluorescence etc. can be observed which is the resultant of chemical contact, excited-state reaction, energy transfer, and complex formation which contribute to the above-mentioned phenomena. Thus CDs are potential precursors because of its excellent optical qualities, robust absorption, intense luminescence [35], and excellent light stability and hence has wide application in the field of biosensors [25, 36–39] in biomedicine [40], metal sensing [31, 41–43] catalysis [44], as light-emitting diodes [45], in dye degradation [46] latent fingerprint sensing [47, 48] etc. The continual persuasion of benign synthetic pathways is fuelled by a plethora of intriguing precursors found in nature [49]resulting in green synthetic procedures to obtain CDs [2, 50–54]. The objective of the study is i) to detect MPs from cosmetic cleansers using CDs obtained from environmentally friendly green source ii) identify the mechanism responsible for the detection of MPs iii) study the degradation of surgical face mask over a period of time and iv) apply CDs to detect MPs released from surgical facemask.

The resin obtained from the plant *Araucaria Araucana (common name-Monkey Puzzle tree)* is used for the synthesis

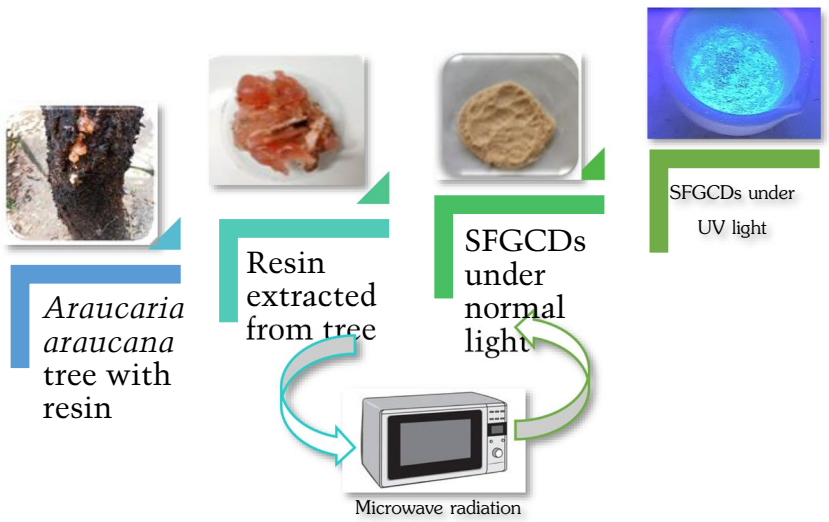

Fig. 1 One pot synthesis of SFGCDs from *Araucaria araucana* resin

of carbon dots because, i) There are no reports yet in earlier literature where the resin from this tree is been used as a source for the synthesis of CDs ii) the resin has a high carbon content in the form of flavonoids, terpenes, saponins, tannins with functional groups present are phenols, carboxyl, carbonyl, hydroxyl as shown in Table S1. Moreover the carbon content in the resin is reported to be nontoxic [55, 56] we chose this resin for the synthesis of CDs.

The Identification and quantification of MPs using CDs from a plant resin, *Araucaria araucana* (Monkey Puzzle tree) by an environment-friendly microwave method is reported here. The detection of MPs in cosmetic personal cleansers by naked eye using CDs as the probe by simple PL technique is conducted and based on the detection ability of the probe, the CDs are applied to detect MPs in the form of fibres released from disposable surgical facemasks in water.

Materials and Methods

Materials

The precursor for the synthesis of CDs a resin from an indigenous gymnosperm *Araucaria araucana* commonly called "monkey puzzle tree" found in Kanyakumari district, Tamil Nadu, India. Source of MPs -Disposable Surgical face masks purchased from Pharmacy, Cosmetic personal Cleansers containing microbeads/ MPs purchased from cosmetic products outlet. Double distilled water is used for immersing the surgical face mask for the degradation studies.

Instrumentation

UV–Vis spectra is recorded using Perkin Elmer Lambda 35 UV/Visible spectrometer in the range 400-800 cm^{-1}. SEM–EDX response is studied using FEI-Quanta FEG 200F with high resolution. Fourier Transform Infrared (FTIR) spectra is measured using The Perkin Elmer Spectrum1. FT-IR spectrometer consisting of globar and mercury vapor lamp as source to study the entire IR region of 450-4000 cm^{-1}. X-ray diffraction studies is done using BRUKER D8 VENTURE SC-XRD system with Cu-Kα radiation. PL analysis is carried out using Spectro fluorimeters—Horiba (DST-PURSE) and Varian (UGC-UPE).

Synthesis of CDs

CDs is synthesized from natural resin obtained from *Araucaria araucana* using facile one pot microwave assisted hydrothermal, environment-friendly, green method. The synthesis represented in (Fig. 1) is carried out by dissolving 5 g of resin in 25 ml double distilled water and heated in a domestic 800W microwave oven for 20 min. The synthesized pale brown coloured CDs is centrifuged at 5000 rpm for 30 min, the residue is dried, ground using motor and pestle. The obtained CDs are solid, sand coloured under visible light and exhibit green fluorescence under UV radiation and final product is named as Solid Fluorescent Green Carbon Dots (SFGCDs). 0.1 g of SFGCDs is utilized throughout the study.

Extraction and Detection Procedure of Microplastics

Cosmetic personal cleanser is dissolved in hot water, the resultant solution is filtered using Whatman filter paper of pore size 6 µm. The residue obtained is MPs in bead form, which is mixed with SFYCDs and used for the selective detection studies. Similarly, a new disposable surgical face mask is purchased from the pharmacy, immersed in

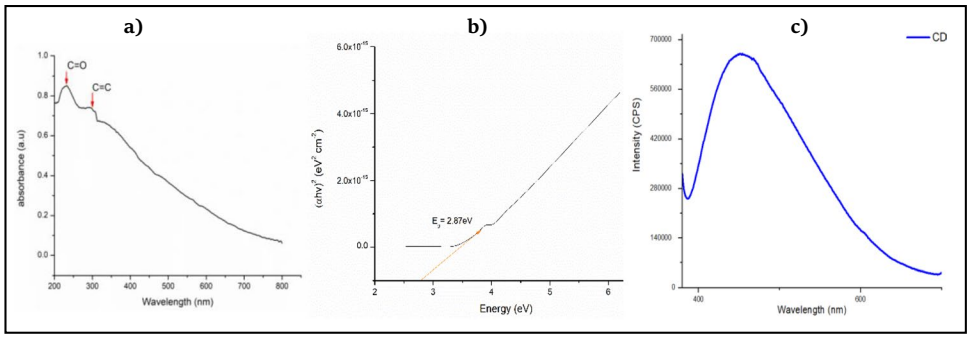

Fig. 2 **a**) UV response of SFGCDs **b**) Tauc plot **c**) PL response of synthesized SFGCDs

double distilled water (distilled water is used to prevent the effect of monovalent and divalent ions in the study) and the degradation of the mask is studied for a period of 50 days ie. Responses was noted on the 30th, 45th and 50th day. Detection of MPs is done by addition of SFYCDs to the water containing MP fibres. The detection of MPs released from cosmetic cleanser and surgical face mask in water is analysed using PL studies.

Results and Discussion

The one-pot synthesis of SFGCDs using microwave method from plant resin is a low-cost, non-toxic and eco-friendly technique. It is observed, the synthesized SFGCDs does not exhibit fluorescence in presence of visible light, whereas it shows green fluorescence in presence of UV light (Fig. 1). In presence of UV light, some of the electrons in CDs get enough energy, gets excited, breaks out from the atoms permitting them to travel around the CDs forming a conduction band where electrons are free to flow through the material. When these electrons return to the atom's outer orbit (the valence band), they emit light. The energy difference between the conduction band and the valence band results in green fluorescence [57].

Optical Studies – UV–Vis and PL Spectral Analysis of SFGCDs

The optical property of the synthesized SFGCDs is confirmed by UV–Vis and PL spectral analysis. CDs derived from plant sources usually have a strong peak in the UV region with its tail extended into the visible area confirming the presence of low energy surface centres related to functionalization of CDs. The peaks in Fig. 2a confirms the presence of Aromatic π orbitals due to the formation of graphitic carbon structure [58]. The peak at 250 nm is due to the $\pi \rightarrow \pi^*$ transition of C = C bond, at 343 nm due to $n \rightarrow \pi^*$ transition of the C = O bond [59] respectively confirming the presence of 15-acetoxylabd-8(17) en-19-ol,15,19diacetoxylabd-8(17) en and 24 diterpenes [60, 61] in SFGCDs. Tauc plot Fig. 2b confirms the band gap of SFGCDs is 2.8 eV which is due to quantum confinement effect and radiative recombination of the surface-confined electrons and holes [62–65]. Figure 2c represents the PL spectrum of SFGCDs with the emission wavelength at 474 nm on excitation at 350 nm, confirming plant-based CDs show maximum emission at excitations between 350 and 370 nm.

The peak in the PL is associated with the recombination of electron–hole pairs and band-to-band transitions. The conjugated aromatic systems, ascorbic acid, polysaccharides, esters, carboxylic acid, terpenoids, and carbohydrates are responsible for the green fluorescence of SFGCDs [66, 67]. While synthesizing SFGCDs, conjugated aromatic systems are formed and eventually emission states arise on the surface of SFGCDs. CDs that emit green light with long wavelengths are of great significance for extending the light-absorption ranges and realizing the effective utilization of light [68]. The green fluorescence corresponds to n–π* transitions of the edge states [69–71]. The observed PL response due to bandgap (HOMO–LUMO) transitions correspond to conjugated π-domains [72]. Thus, the fluorescent nature of SFGCDs arise due to band gap transitions,

Morphological Characterization of SFGCDs –XRD, FTIR, SEM-EDAX, TEM Analysis

Figure 3a shows a broad, sharp, single XRD peak of SFGCDs centred at $2\theta = 21°$confirming the presence of graphitic carbon, amorphous in nature with an interplanar spacing of 0.45 nm, which is nearly equal to the spacing between (002) planes in bulk graphite (3.34). A wider lattice spacing (0.37 nm) of SFGCDs than ordinary bulk graphite (0.34 nm) indicates partial crystallization and considerable graphitization. The partial degree of crystallization/graphitization in SFGCDs might be due to their partial turbostatic carbon structure [73] and densely packed oxygen-bearing functional groups on the surface. The crystalline size calculated using Debye- Scherrer equation demonstrate to be 3.16 nm proving SFGCDs as nanoparticles [74]. Scherrer

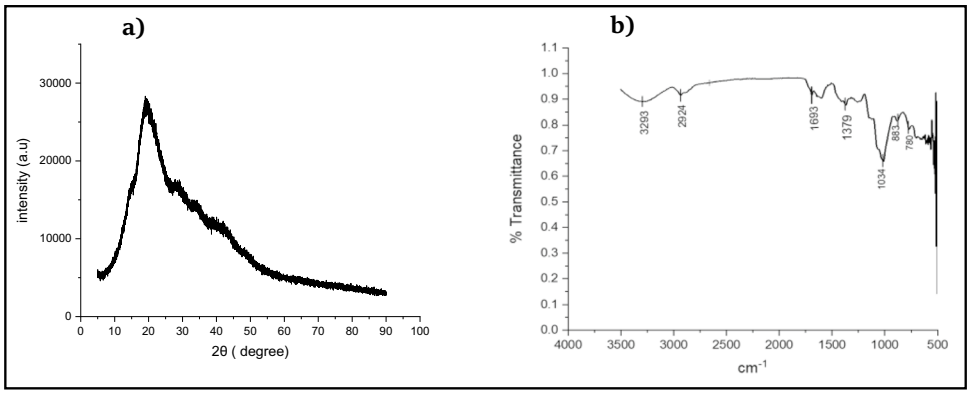

Fig. 3 **A** XRD pattern of synthesized SFGCDs **b** FTIR spectrum of synthesized SFGCDs

equation $D = K\lambda / (\beta \cos \theta)$ where D is the average thickness in the vertical direction of the crystal face, K—Scherrer constant = 0.89, λ the wavelength of X-ray, β the half-high width of the diffraction peak of the sample, and θ being the diffraction angle(deg).

The FTIR response (Fig. 3b) of the synthesized SFGCDs shows intense peak around 1034 cm^{-1} in the fingerprint region confirming the presence of -OH functional group. The prominent peak at 1693 cm^{-1} is due to C = O stretching, peak around 2924 cm^{-1} and broad band from 3000 cm^{-1} to 3293 cm^{-1} attributed to C-H, O–H stretching. Similarly, the peak at 1379 cm^{-1} contributes to O–H bending at the fingerprint region. Further, the peak at 883 cm^{-1} corresponds to the geminal disubstituted C = C and the peak at 780 cm^{-1} is due to meta-disubstituted benzene compounds. Thus, FTIR examination reveals the presence of carboxyl, ketone, ester, and alcohol groups on the surface of the synthesized SFGCDs sp^2 /sp^3 core carbon [65]. The presence of increase in carbon content and functional groups on the surface of SFGCDs is responsible for their superior green photoluminescence nature which corroborates with earlier literature authenticating [60, 61] the presence of 15-acetoxylabd-8 (17) en-19-ol, 15,19-diacetoxylabd-8 (17) en-19-ol, and 24 diterpenes in the resin.

The SEM- EDX image (Fig. 4a) of SFGCDs depict uniformly sized cubical structure confirming the synthesized SFGCDs are enriched with a high Carbon matrix authenticating the presence of only Carbon and Oxygen and absence of Nitrogen or other elements. Moreover, the EDAX measurements of SFGCDs are in agreement with the FTIR data and the qualitative analysis Table S1 emphasizing the presence of only C = O, COOH, O–H functional groups. The TEM image Fig. 4b of SFGCDs shows lattice spacing value of 0.44 nm. The weak and broad diffuse rings in the SAED pattern (Fig. S1) confirms amorphous nature [75] corresponding to the basal plane distance of graphite with the existence of several well-defined lattice fringes, evenly dispersed in SFGCDs with an average size of 3.63 nm which is in good agreement with the XRD results.

Detection of Microplastics (MPs) from Cosmetic Personal Care Cleansers & Disposable Surgical Mask in Water Using SFGCDs

The simple naked eye detection of MPs from water is based on the fluorescent property of SFGCDs and the hydrophobic nature of MPs in aqueous environment. Detection of MPs by the fluoroprobe is clearly explained based on the variations observed in the optical property, FTIR, SEM response of SFGCDs,

Detection of MPs Released from Cosmetic Cleansers

The UV–Vis response of SFGCDs in presence of MPs from Cosmetic Cleansers Fig. 5a, shows a peak at 213 nm. Aa shift of the response towards lower wavelength (red shift) with increase in intensity compared to 343 nm for bare SFGCDs (Fig. 2a) confirm the presence of MPs and also substantiates the increase in carbon content on the surface of SFGCD matrix. Figure 5b shows a small decrease in band gap of 2.3 eV compared to bare SFGCDs. The PL response Fig. 5c shows decreased intensity of 1,20,000cps with an hypsochromic shift to 370 nm compared to 474 nm and 6,80,000cps intensity of bare SFGCDs (Fig. 2c) with a TURN OFF in fluorescence. The above observations confirm the presence of MPs on the SFGCDs matrix. The increase in carbon content in the form of polyethylene agglomerated on the surface of SFGCDs forbids electron- hole recombination resulting in TURN- OFF Fluorescence.

TURN OFF in fluorescence, a consequence of the presence of MPs on the surface of SFGCDs, is further established by the SEM- EDX response. Figure 6 Clearly shows the agglomeration of MPs on the surface of SFGCDs. The agglomeration of MPs function as an insulator thereby forbidding electron- hole recombination between the valence band and conduction band of SFGCDs. Similarly, as MPs cover the surface of SFGCDs a change in the morphology of CDs is clearly observed from the SEM response (Fig. 6). The observed change in morphology is the reason for the

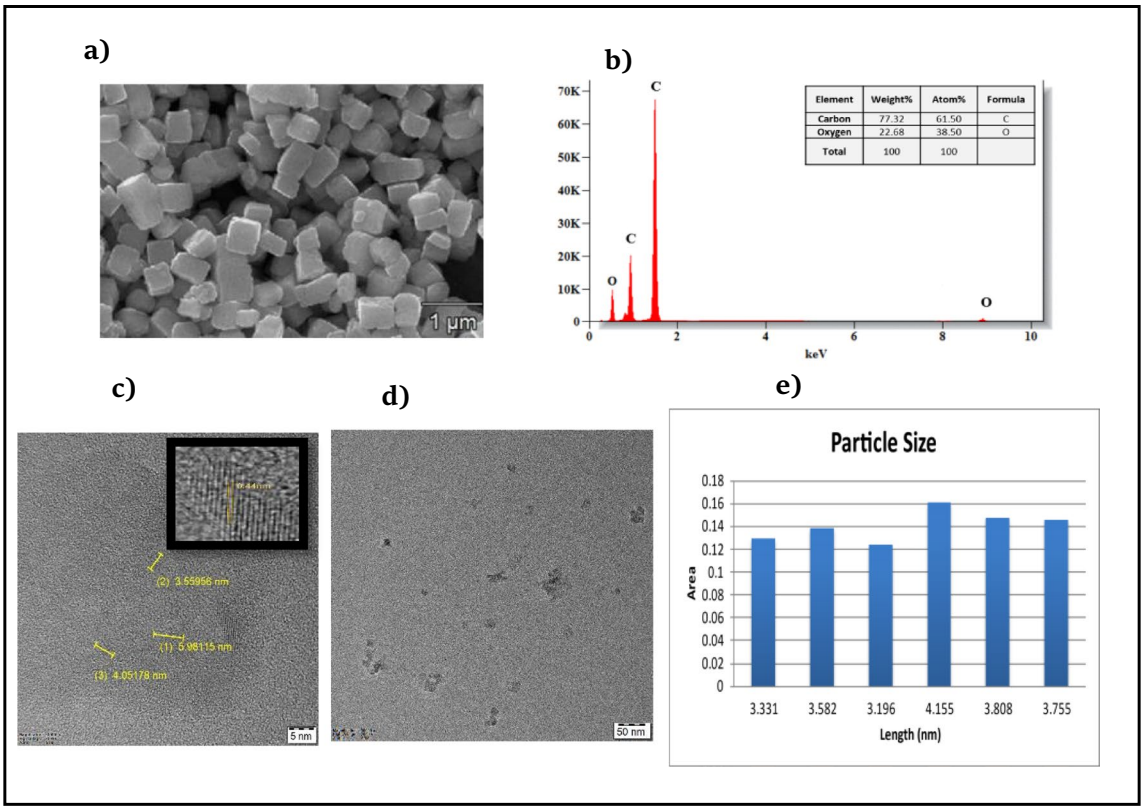

Fig. 4 **a**) SEM **b**) EDX image of SFGCDs **c**) TEM images of SFGCDs Inset: Lattice spacing value calculated from HR-TEM image **d**) 50 nm magnification of TEM image **e**) particle size distribution

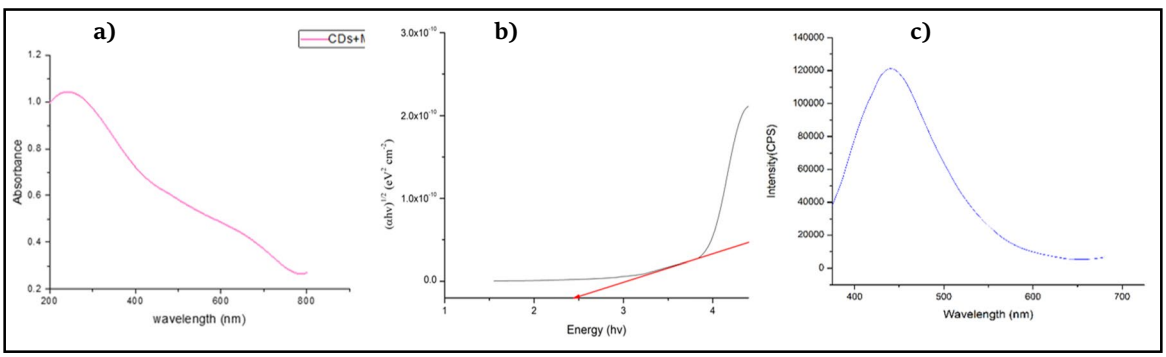

Fig. 5 **a**) UV-Vis response of SFGCDs in presence of MPs (**b**) Tauc plot **c**) PL response SFGCDs in presence of MPs

TURN OFF in fluorescence. Further, Fig. 6- EDAX response also clearly points the increase in carbon content due to agglomeration of MPs on the surface of SFGCDs which further substantiates the presence of MPs i.e. hydrophobic polymers like PE, PP, polyvinyl chloride (PVC), polystyrene (PS), polyamide (PA) and PET [7, 8]on the surface of SFGCDs. Thus, the decrease in PL intensity with Turn OFF in fluorescence of SFGCDs in presence of MPs as observed in Fig. 5c affirm the detection ability of MPs by SFGCDs.

Further, the type of polymer responsible for the Turn-Off in Fluorescence of SFGCDs is confirmed by the FTIR response Fig. 7a &b. Figure 7a is the FTIR spectra of pure MPs extracted from personal cosmetic cleansers. The prominent peak at 3377 cm^{-1} is due to O–H stretching and the peaks around 1618 cm^{-1} and 1721 cm^{-1} are attributed to C = O and C = C stretching proving the MPs contain polyethylene group. Figure 7b shows the FTIR response of MPs on SFGCD matrix. It clearly shows the broadening of O–H

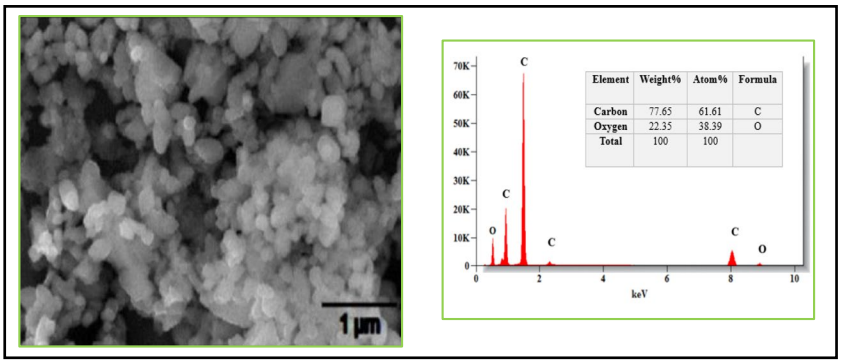

Fig. 6 SEM- EDAX image of SFGCDs agglomerated with MPs

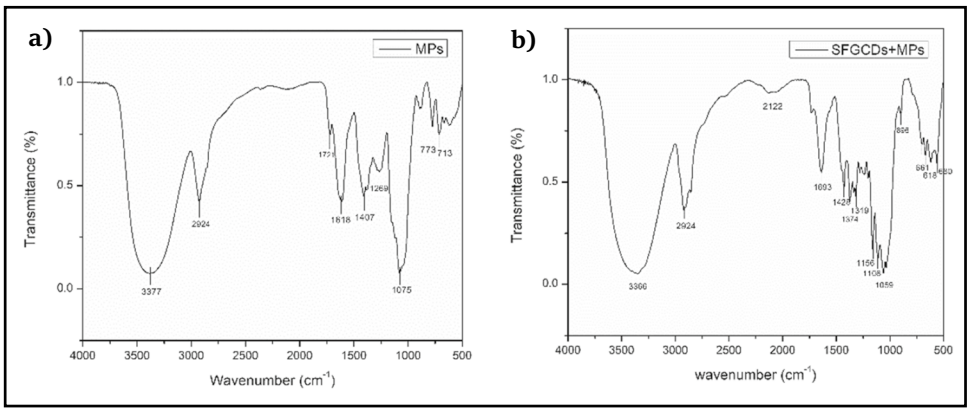

Fig. 7 **a**) FTIR spectrum of MPs from personal cleanser **b**) FTIR spectrum of SFGCDs + MPs

peak of SFGCDs and additional signals at lower wavelength region 1693 cm^{-1},1374 cm^{-1}, 880 cm^{-1} are observed compared with the FTIR spectra of bare SFGCDs (Fig. 3b). Henceforth, it confirms SFGCDs matrix is covered by only Polyethylene MPs, which results in Turn OFF in fluorescence of SFGCDs [76].

Effect of Concentration of MPs on the Detection Ability of SFGCDs

Figure 8a depicts the decrease in PL intensity of SFGCDs with increase in addition of MP's (0.1 g, 0.5 g, 1 g, 2 g). Thus, it is a clear proof that SFGCDs functions as an efficient fluoroprobe towards detection of MPs. The hypsochromic shift followed by decrease in PL intensity of SFGCDs with increase in concentration of MPs (Fig. 8a) electron acceptor insulator molecules i.e., the polyethylene MPs which cover the surface of SFGCDs. Since the quenching molecules (MPs) are poor electron donors, electron transfer is forbidden between the valence band and conduction band of SFGCDs which results TURN OFF in fluorescence of SFGCDs. Increase in concentration of MPs onto the SFGCD matrix leads to their agglomeration on the surface resulting in surface passivation. We know that the photoluminescence in CDs is due to the radiative recombination of the surface-trapped electrons and holes [77]. The carbon core of SFGCDs is very small which creates a homogenous particle surface. The agglomeration of organic polymer functional groups on SFGCDs disrupts radiative recombination resulting Turn-Off in Fluorescence. Figure 8b the Stern Volmer plot shows a linear relation between I_0/I and the increase in weight of MPs ranging from 0.1 to 2 g through a linear regression equation

$$I_0/I = 0.0011[MPs] + 0.932$$

confirming Dynamic quenching mechanism being responsible for the detection of MPs. The values of the correlation coefficient ($R^2 = 0.99$) clearly indicate the effect of linearity of the system. The minimum limit of detection of MPs by SFGCDs probe is calculated to be 0.0063 g/l using standard deviation.

Proposed Mechanism for Detection of MPs

The stern- Volmer Plot Fig. 8b confirms Dynamic quenching mechanism as responsible for detection of MPs. Further Fig. 9 explains the FRET mechanism responsible for quenching. Figure 0.6. SEM- EDX response, Fig. 7b. FTIR response & Fig. 8a confirms the MP is agglomerated on the surface of SFGCDs resulting in effective quenching in green fluorescence. Thus, the quench in fluorescence with

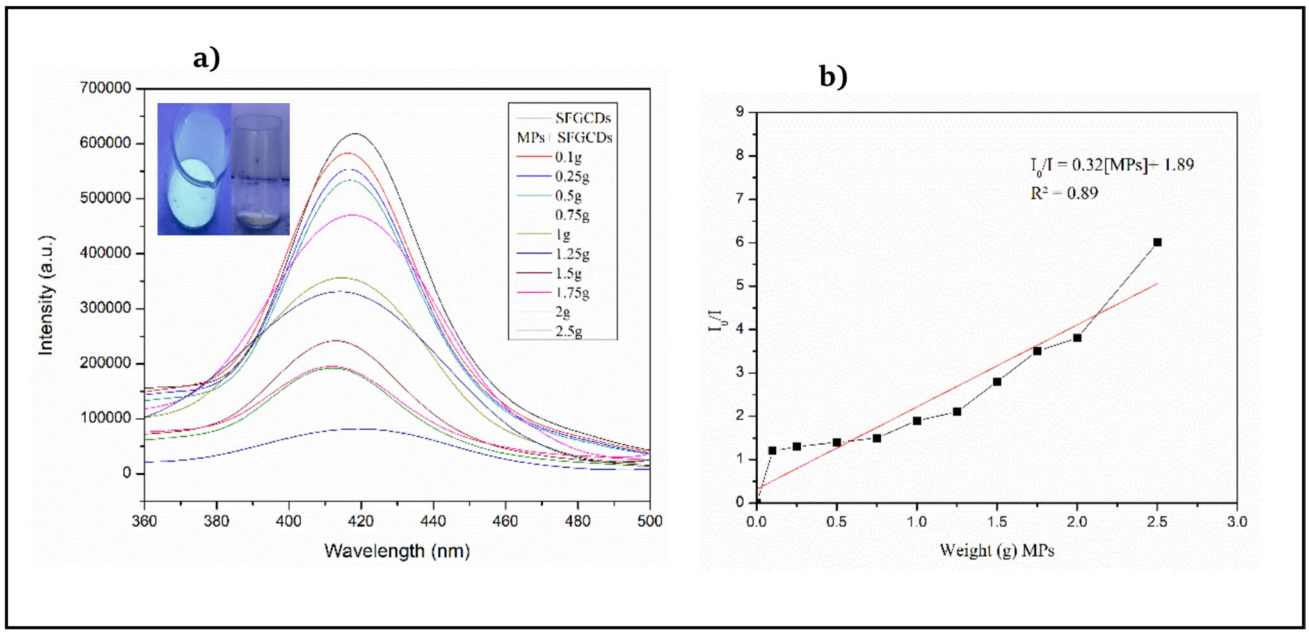

Fig. 8 (**a**) PL response with increase in addition of MPs to SFGCDs Inset: Before and after addition of MPs (**b**) Stern Volmer plot

increase in addition of MPs is due to the binding of electron acceptor MPs onto the surface of SFGCDs, resulting in trapping of excited electrons and hence Turn Off in fluorescence. Similarly, from Fig. 8a it is clearly observed, increase in addition of MPs broaden PL response of SFGCDs, the energy available for emission gets essentially depleted when MPs agglomerate on the surface of SFGCDs with a reduced ability to excited state (FRET). A consequence observed with decrease in fluorescence intensity and decrease in transmittance percentage [78] Fig. 7b. Thus, it is clear that MPs quench the radiative emission by effectively blocking electron- hole (charge) recombination, thereby enabling SFGCDs to function as an easy and effective fluorescent probe towards detection of MPs. As the MPs are released from the surface of SFGCDs, the FRET between SFGCDs and MPs is terminated and fluorescence reappears which explain the remediation of MPs [79].

Detection of Microplastics Released from Unhealthy Disposal of Surgical Facemask in Water

During and after the COVID 19 pandemic, careless disposal of used surgical face mask remains as a treat to the environment. Various types of masks like surgical or medical, FFP2, N95, cotton, and activated carbon masks are being used by common man since the Covid-19 pandemic [80].The primary source of increase in synthetic and natural microfibres in freshwater after the COVID 19 pandemic is due to the careless disposal of single use, reusable surgical facemask. Inappropriate and unhealthy practices of disposing surgical mask results in accumulation of MPs in land, water and air. Poly propylene and plasticizers in surgical mask break down to plastics in the environment. The plastics from surgical facemasks further breaks down into Microfibre/MPs when exposed to UV radiation, mechanical stress or even hydrolysis.

In the current study, the degradation of a single use surgical facemask in DD water is studied for a period of 30, 45 and 50 days. Based on the detection ability of MPs by SFGCDs from the above study, SFGCDs are applied towards the detection of MPs released from facemask. atactic polypropylene [81], polyamide, polyethylene or phthalates are the forms of MPs which are released from the surgical facemasks [82, 83]. Studies indicate that the careless disposal of face masks in the environment results in the formation of mean $2.1 \pm 1.4*10^{11}$ pieces/m^2 of mask. [84, 85]. The total number of microplastics released from surgical mask can be calculated using the formula [83], $N = C_a / A_i * A_T$, N = Total no. of microplastics, C_a = Average amount of microplastic in image, A_i = Image area, A_T = Total area of the filter membrane.

The filtered microfibres are then placed separately in an aluminium foil for morphological analysis (Fig. 10). Figure 10a shows the photograph of the degraded surgical mask on the 50th day. The SEM picture (Fig. 10b &c) depicts the fibres released from the surgical mask since 15th day. It confirms the degradation nature of mask in water, which shows the intensity of danger due to MPs to the aquatic environment in specific and to the ecosystem by large. Fig S2 depicts the FTIR response of MP fibres from surgical

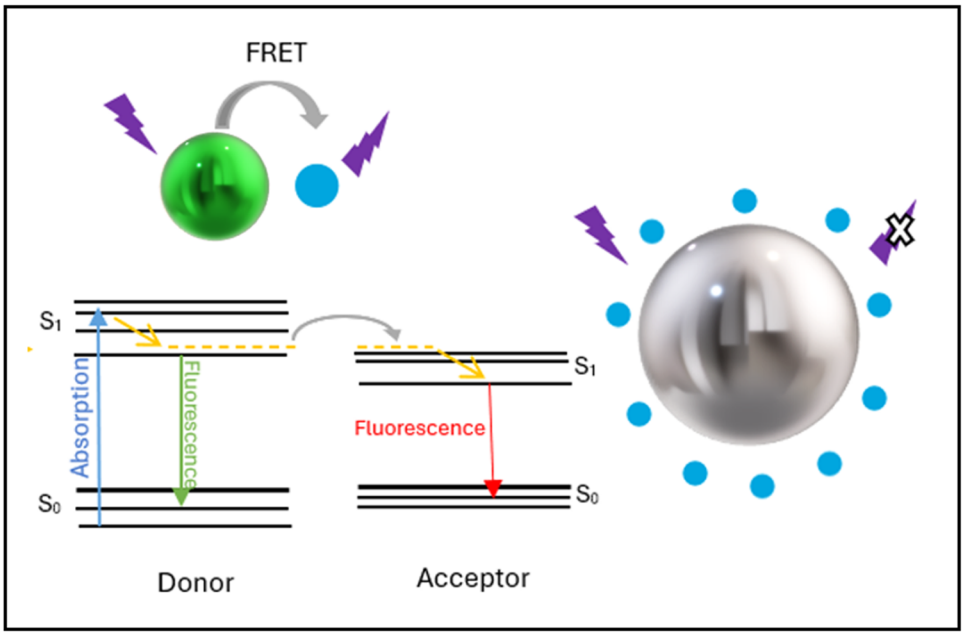

Fig. 9 Dynamic quenching mechanism in SFGCDs to detect microplastics

face mask which confirming the presence of polyester and polypropylene.

Samples were collected on the 30th day, 45th day and 50th day. Figure 11a confirms degradation of surgical mask in water with MP fibres from the masks released into water. For the experimental investigation, 1 ml of water containing microfibres (30th day sample) and 0.1 g of SFGCDs are stirred for 30 min. Figure 11b clearly shows the decrease in PL intensity of SFGCDs with TURN OFF in fluorescence, confirming presence of MPs on the surface of SFGCDs. The continuous decrease in fluorescence with the increase in concentration of microfibres released into water with the degradation of mask on the 30th, 40th and 50th day confirms that, as days pass by from 30th day to 50th day, the amount of microfibres released into water increased and a decrease in PL intensity with broadening of PL response, a shift of the PL peak towards lower wavelength confirming increased concentration of microfibre/MP.

The microfibres made up of polypropylene and plasticizers consist of conjugated alkenes. The agglomeration of microfibres on the surface of SFGCDs reduce the band gap of SFGCDs. Since MPs function as an insulator, their presence on the surface of SFGCDs forbid electron–hole recombination between the conduction band and valence band, as observed in presence of cleansers. The energy available for emission gets essentially depleted when MPs agglomerate on the surface of SFGCDs which results in the reduced ability to transfer energy from SFGCDs to MPs in an excited state (FRET), a consequence observed with fluorescence intensity getting lowered. But, when the microfibre solution was filtered using Whatman filter paper having pore size 6 µm SFGCDs regained its fluorescence confirming easy electron

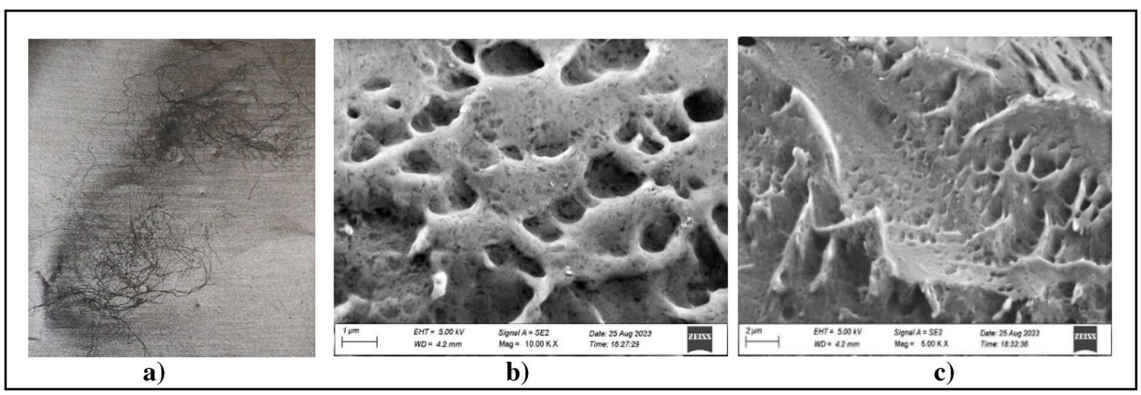

Fig. 10 **a**) Photograph of surgical face mask on the 50th day in aqueous environment. **b** & **c**) SEM image of microfibres released from surgical face mask

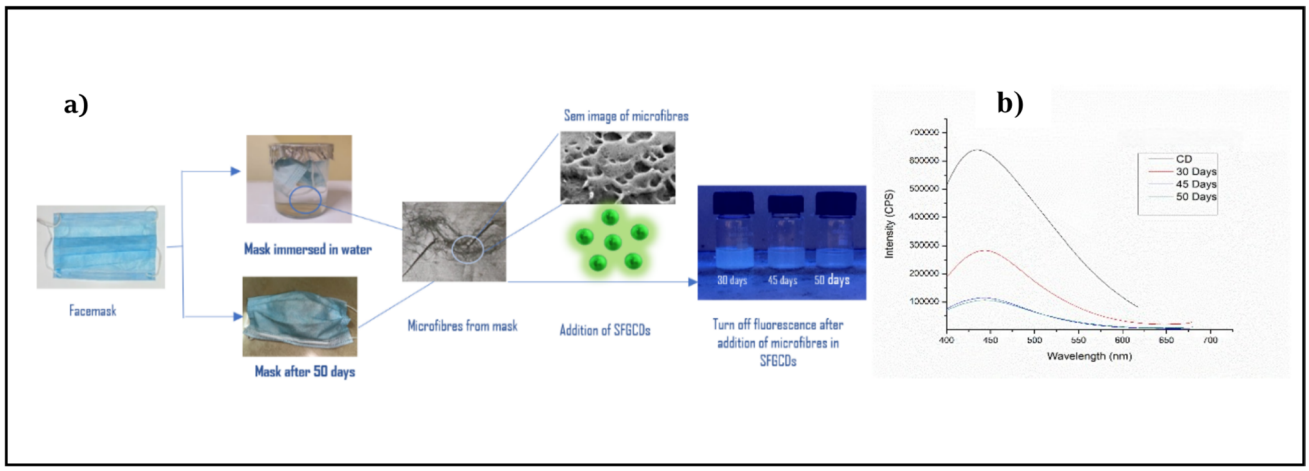

Fig. 11 (**a**) Experimental setup for analysing microfibres released from surgical facemask (**b**) Decrease in PL intensity of SFGCDs with increase in addition of MPs

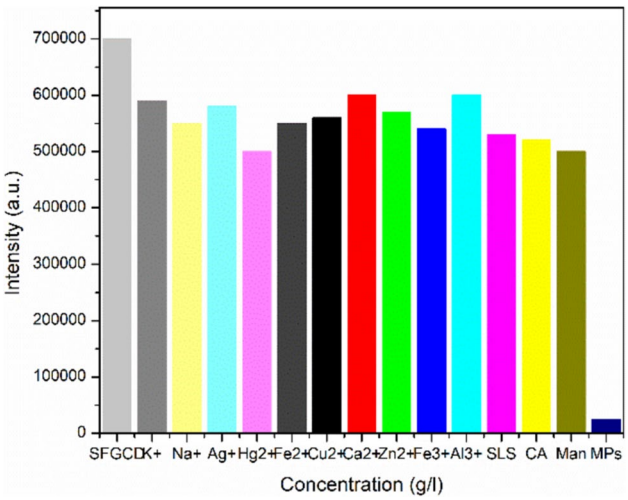

Fig. 12 Bar graph representing the selective detection of MPs in presence of interfering monovalent, divalent, trivalent ions and biomolecules (SLS-Sodium Lauryl sulphate, CA-citric acid, Man-Mannitol)

– hole recombination between the valence band and conduction band of SFGCDs.

Selective Detection of MPs

Figure 12 shows the selective detection of MPs in presence of interfering monovalent (Na^+, Ag +) divalent (Zn^{2+}, Hg^{2+}, Fe^{2+}, Cu^{2+}) trivalent (Al^{3+}, Fe^{3+}) ions and biomolecules (mannitol, Citric Acid, Sodium Lauryl Sulphate (SLS) molecules of cosmetic cleansers, surgical facemask and ions present in water. The result confirms that the background inferences and false positive signals are avoided by using the turn-on or off luminescence approach and reflect actual circumstances when working with real samples [86]. The exceptional optical properties of SFGCDs with no extra peaks in the PL response prove it as an effective and sustainable tool towards Identification and quantification of Microplastics. Table S2 clearly substantiates the novelty of SFGCDs to detect MPs with the lowest detection limit reported till date by a simple naked eye technique compared to the earlier reported methods.

Remediation of MPs Using SFGCDs

Figure 13 clearly depicts the remediation of MPs by simple separation method. Figure 13 clearly depicts 0.1 g additions of microplastics from personal cleansers to SFGCDs results in TURN OFF in fluorescence in presence of UV light. When the mixture of SFGCD and MPs are separated by a simple filtration using Whatman filter paper of pore size 6 µm fluorescence of SFGCDs TURNS ON as shown in Fig. 13c. Figure 13d depicts the PL response in presence of 2 g of MPs and after remediation of MPs. The PL intensity of SFGCDs increases to 500000au with remediation of MPs. An increase in fluorescence intensity with shift of emission peak back to higher wavelength (bathochromic shift) 473 nm similar to bare SFGCDs confirms the remediation of MPs from aqueous environment. Further, the increase in PL intensity signifies reoccurrence of radiative recombination of electron—hole leading to TURN ON in fluorescence in SFGCDs (FRET). Thus, the synthesised SFGCDs functions as a versatile fluoroprobe. A recent study also proved the affinity of carbon nanomaterial towards microplastics [87, 88]

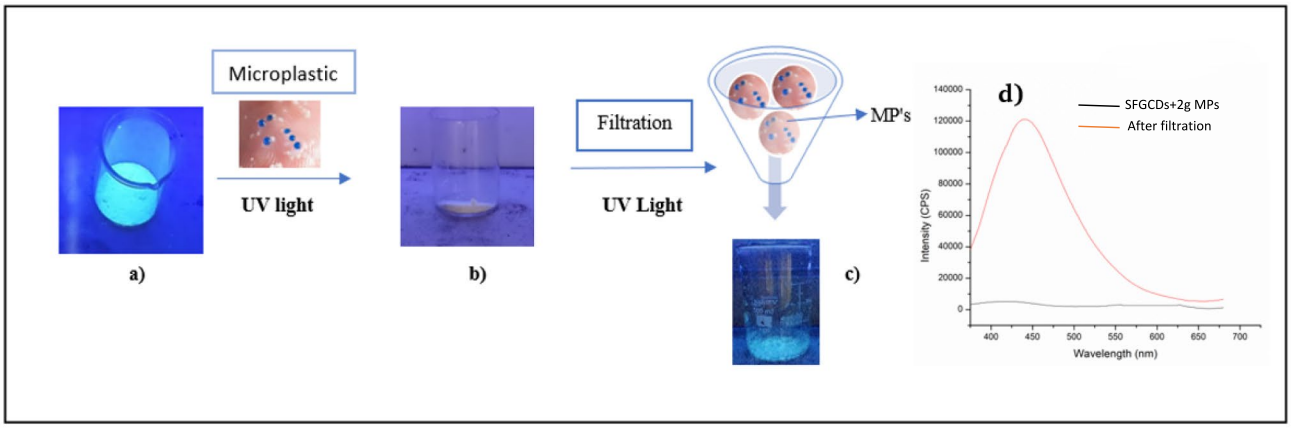

Fig. 13 Pictorial representation of remediation of microplastics a) SFGCDs b) TURN OFF fluorescence of SFGCDs in presence of MPs c) TURN ON Fluorescence in SFGCDs with remediation of MPs d) PL response of SFGCDs in presence and absence of MPs

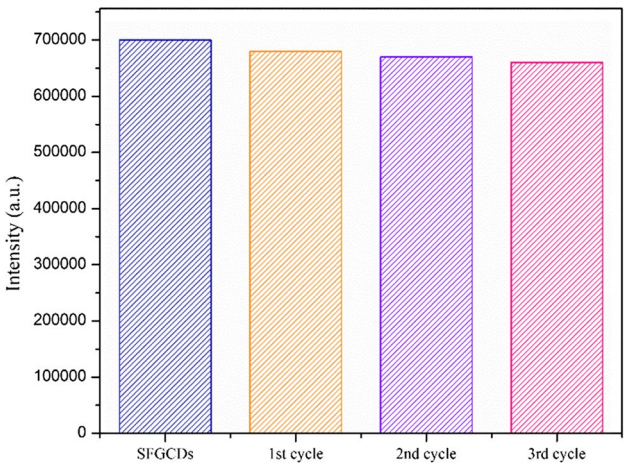

Fig. 14 Reusability of SFGCDs up to 3 cycles

Stability of SFGCDs

SFGCDs as they are insoluble in water can be recycled multiple times for the detection of MPs. Figure 14 confirms SFGCDs can been reused nearly 3 times continuously for the detection and remediation process wherein the PL intensity of SFGCDs remains the same. Further, as i) only 0.1 g of SFGCDs is used for detection of MPs ii) SFGCDs are reused and recycled, the whole process helps in reducing carbon footprint and sustaining a safe aqueous environment.

A drawback observed during the remediation process of MPs is, the Whatman filter paper used for remediation can be used only once. Our future studies are i) to analyse if the SFGCDs agglomerated with the microparticles can be modified into a composite to construct energy storage device ii) construct environmentally friendly reusable filters with less than 6 µm pore size for remediation of nano plastics.

Conclusion

In summary, SFGCDs is synthesised for the first time from the resin of *Araucaria araucana* through microwave approach. The synthesised SFGCDs is non-toxic as the precursor is a resin of natural origin and exhibits green fluorescence. The formation of SFGCDs is confirmed by the PL, UV–Vis absorption peak, SEM-EDAX, HR-TEM, FTIR and XRD measurements confirming amorphous, cubic morphology, presence of only carbon and oxygen with a particle size of 3.63 nm. The synthesised SFGCDs was applied towards selective detection and remediation of MPs released from personal cosmetic cleansers and disposable surgical mask. In presence of MPs, the dynamic quenching mechanism leads to TURN OFF in fluorescence of SFGCDs confirmed by Stern- Volmer plot. The decrease in intensity is due to forbidden electro- hole recombination between the valence band and conduction band and agglomeration of MPs on the surface of SFGCDs. Thus, SFGCDs function as a template towards detection of MPs. A simple filtration technique helps in remediation of MPs above 6 µm size with a detection limit of 0.0064 mg/l. The application of the fluoroprobe is studied towards detection of micro fibres released from surgical face mask which are disposed in water bodies. The degradation of surgical facemask at regular intervals of time to nanofibers is studied and the detection of the same using SFGCDs is clearly explained in the current work. The selective detection of MPs in presence of monovalent, divalent, trivalent ions, biomolecules and the reuse of SFGCDs only for 3 consecutive cycles confirming the stability of SFGCDs.

Supplementary Information The online version contains supplementary material available at https://doi.org/10.1007/s10895-025-04152-x.

Acknowledgements The authors acknowledge the Department of Chemistry, Madras Christian College for the support. We also acknowledge the assistance with instrumentation techniques provided

by SRM-NRC Kattankulathur- Chennai, GNR instrumentation UNOM-Chennai, and IIT Madras.

Author Contribution CRediT: **Ayun R Jini –** Data curation, Formal analysis, Investigation, Methodology, Resources, Software, Writing- original draft**. G. Gnanamani Simiyon-** Resources **T. Mary Vergheese** – Conceptualization, Investigation, Methodology, Resources, Supervision, Validation, Writing- review & editing.

Declarations

Conflicts of Interest There are no conflicts to declare.

References

1. Courtney A, Joel B, Holly B. Proceedings of the international research workshop on the occurrence, effects, and fate of microplastic marine debris. NOAA technical memorandum, September, pp 9–11. https://repository.library.noaa.gov/view/noaa/2509/noaa_2509_DS1.pdf
2. Wang X, Feng Y, Dong P, and Huang J (2019) A mini review on carbon quantum dots: preparation, properties, and electrocatalytic application. Catal Photocatal 7
3. Guo J-J et al (2020) Source, migration and toxicology of microplastics in soil. Environ Int 137
4. Queiroz AFDS et al (2022) First assessment of microplastic and artificial microfiber contamination in surface waters of the Amazon continental shelf. Sci Total Environ 839
5. Mu H et al (2022) High abundance of microplastics in groundwater in Jiaodong Peninsula, China. Sci Total Environ 839. https://doi.org/10.1016/j.scitotenv.2022.156318
6. Gaylarde CC, Baptista Neto JA, and Da Fonseca EM (2021) Nanoplastics in aquatic systems - are they more hazardous than microplastics? Environ Pollut 272:115950. https://doi.org/10.1016/j.envpol.2020.115950.
7. Zhu K et al (2019) Formation of environmentally persistent free radicals on microplastics under light irradiation. Environ Sci Technol 53(14):8177–8186. https://doi.org/10.1021/acs.est.9b01474
8. Randhawa JS (2023) Advanced analytical techniques for microplastics in the environment: a review. Bull Natl Res Cent 47(1):174. https://doi.org/10.1186/s42269-023-01148-0
9. Sheng X, Wang J, Zhang W, Zuo Q (2021) The potential for PE microplastics to affect the removal of carbamazepine medical pollutants from aqueous environments by multiwalled carbon nanotubes. Toxics 9(6):139
10. Abuwatfa WH, Al-Muqbel D, Al-Othman A, Halalsheh N, Tawalbeh M (2021) Insights into the removal of microplastics from water using biochar in the era of COVID-19: a mini review. Case Stud Chem Environ Eng 4
11. Maes T, Jessop R, Wellner N, Haupt K, Mayes AG (2017) A rapid-screening approach to detect and quantify microplastics based on fluorescent tagging with Nile Red. Sci Rep 7:44501
12. Padervand M, Lichtfouse E, Robert D, and Wang C (2020) Removal of microplastics from the environment. A review. Environ Chem Lett 18:s807–828
13. Singh S, Kalyanasundaram M, Diwan V (2021) Removal of microplastics from wastewater: available techniques and way forward. Water Sci Technol 84(12):3689–3704. https://doi.org/10.2166/wst.2021.472
14. Chomiak KM, Eddingsaas NC, Tyle AC (2023) Direct and indirect impacts of disposable face masks and gloves on freshwater benthic fauna and sediment biogeochemistry. ACS EST Water 3(1):51–59. https://doi.org/10.1021/acsestwater.2c00358
15. Zhou Y et al (2023) Current research trends on cosmetic microplastic pollution and its impacts on the ecosystem:a review. Env Pollut 320.
16. Mohamed Nor NH, Kooi M, Diepens NJ, and Koelmans AA (2021) Lifetime accumulation of microplastic in children and adults. Env Sci Technol 55(8):5084–5096
17. Yan Z, Liu Y, Zhang T, Zhang F, Ren H, Zhang Y (2022) Analysis of microplastics in human feces reveals a correlation between fecal microplastics and inflammatory bowel disease status. Env Sci Technol 56(1):414–421
18. Esperanza Huerta Lwanga et al (2022) Review of microplastic sources, transport pathways and correlations with other soil stressors: a journey from agricultural sites into the environment. Chem Biol Technol Agric 9(20)
19. Nguyen H-HT, Kim E, Imran M, Choi Y-H, Kwak D-H, Ameen S (2024) Microplastic contaminants detection in aquatic environment by hydrophobic cerium oxide nanoparticles. Chemosphere 357. https://doi.org/10.1016/j.chemosphere.2024.141961
20. Faramarzi P, Jang W, Oh D, Kim B, Kim JH, You JB (2024) Microfluidic detection and analysis of microplastics using surface nanodroplets. ACS Sens 9(3):1489–1498. https://doi.org/10.1021/acssensors.3c02627
21. Ahn HM, Park JO, Lee H-J, Lee C, Chun H, Kim KB (2024) SERS detection of surface-adsorbent toxic substances of microplastics based on gold nanoparticles and surface acoustic waves. RSC Adv 14(3):2061–2069. https://doi.org/10.1039/D3RA07382C
22. Qi G, Zhao L, Liu J, Tian C, Zhang S (2024) Single particle detection of micro/nano plastics based on recyclable SERS sensor with two-dimensional AuNPs thin films. Mater Today Commun 38
23. Ruan X et al (2024) Rapid detection of nanoplastics down to 20 nm in water by surface-enhanced raman spectroscopy. J Hazard Mater 462. https://doi.org/10.1016/j.jhazmat.2023.132702
24. Behera A et al (2023) Gold nanoparticle assisted colorimetric biosensors for rapid polyethylene terephthalate (PET) sensing for sustainable environment to monitor microplastics. Environ Res 234. https://doi.org/10.1016/j.envres.2023.116556
25. Song Y et al (2014) Investigation into the fluorescence quenching behaviors and applications of carbon dots. Nanoscole 6:4676–4682
26. Wagner J, Wang Z-M, Ghosal S, Rochman C, Gassel M, Wall S (2017) Novel method for the extraction and identification of microplastics in ocean trawl and fish gut matrices. Anal Methods 9(9):1479–1490. https://doi.org/10.1039/C6AY02396G
27. Majewsky M, Bitter H, Eiche E, Horn H (2016) Determination of microplastic polyethylene (PE) and polypropylene (PP) in environmental samples using thermal analysis (TGA-DSC). Sci Total Environ 568:507–511. https://doi.org/10.1016/j.scitotenv.2016.06.017
28. Araujo CF, Nolasco MM, Ribeiro AMP, Ribeiro-Claro PJA (2018) Identification of microplastics using raman spectroscopy: latest developments and future prospects. Water Res 142:426–440. https://doi.org/10.1016/j.watres.2018.05.060
29. Pirsaheb M, Hossini H, Makhdoumi P (2020) Review of microplastic occurrence and toxicological effects in marine environment: experimental evidence of inflammation. Process Saf Environ Prot 142:1–14. https://doi.org/10.1016/j.psep.2020.05.050
30. Kargbo O, Jin Y, Ding S-N (2015) Recent advances in luminescent carbon dots. Curr Anal Chem 11(1):4–21
31. Mathew A and Mary Vergheese T (2021) N-C dot/Cr (VI)nanoprobe: fluorescent uric acid sensor. Chem Pap 75:5257–5267. https://doi.org/10.1007/s11696-021-01682-z.
32. Georgakilas V, Perman JA, Tucek J, Zboril R (2015) Broad family of carbon nanoallotropes: classification, chemistry, and

applications of fullerenes, carbon dots, nanotubes, graphene, nanodiamonds, and combined superstructures. Chem Rev 115(11):4744–4822
33. Kayani KF, Shatery OBA, Mustafa MS, Alshatteri AH, Mohammed SJ, Aziz SB (2024) Environmentally sustainable synthesis of whey-based carbon dots for ferric ion detection in human serum and water samples: evaluating the greenness of the method. RSC Adv 14(8):5012–5021. https://doi.org/10.1039/D3RA08680A
34. Han Z et al (2019) Highly efficient and ultra-narrow bandwidth orange emissive carbon dots for microcavity lasers. Nanoscale 11(24):11577–11583. https://doi.org/10.1039/C9NR03448J
35. Kayani KF, Ghafoor D, Mohammed SJ, Shatery OBA (2025) Carbon dots: synthesis, sensing mechanisms, and potential applications as promising materials for glucose sensors. Nanoscale Adv 7(1):42–59. https://doi.org/10.1039/D4NA00763H
36. Lu Z et al (2020) A dual-template imprinted polymer electrochemical sensor based on AuNPs and nitrogen-doped graphene oxide quantum dots coated on NiS2/biomass carbon for simultaneous determination of dopamine and chlorpromazine. Chem Eng J 89:124471
37. Ramachandran R, Jini AR, and Vergheese Thomas M (2024) A novel turn-on fluorescence probe for selective picomolar detection of uric acid using green carbon dots (G-NCDs) from waste brachyura shells. Part Syst Charact 2400200. https://doi.org/10.1002/ppsc.202400200.
38. Zu F et al (2017) The quenching of the fluorescence of carbon dots: a review on mechanisms and applications. Microchim Acta 184:1899–1914
39. Kayani KF, Rahim MK, Mohammed SJ, Ahmed HR, Mustafa MS, Aziz SB (2024) Recent progress in folic acid detection based on fluorescent carbon dots as sensors: a review. J Fluoresc. https://doi.org/10.1007/s10895-024-03728-3
40. Farshidfar N, Fooladi S, Nematollahi MH, Iravani S (2023) Carbon dots with tissue engineering and regenerative medicine applications. RSC Adv 13:14517–14529
41. Das P et al (2023) Carbon dots for heavy-metal sensing, ph-sensitive cargo delivery, and antibacterial applications. ACS Appl Nano Mater 3(12):11777–11790. https://doi.org/10.1021/acsanm.0c02305
42. Kayani KF, Abdullah CN (2024) A Dual-mode detection sensor based on nitrogen-doped carbon dots for visual detection of Fe(III) and ascorbic acid via a smartphone. J Fluoresc. https://doi.org/10.1007/s10895-024-03604-0
43. Berchmans S, Vergheese TM, Kavitha AL, Veerakumar M, Yegnaraman V (2008) Electrochemical preparation of copper–dendrimer nanocomposites: picomolar detection of Cu2+ ions. Anal Bioanal Chem 390(3):939–946. https://doi.org/10.1007/s00216-007-1723-z
44. Rosso C, Filippini G, Prato M (2020) Carbon dots as nano-organocatalysts for synthetic applications. ACS Catal 10(15):8090–8810
45. He P et al (2020) Recent advances in white light-emitting diodes of carbon quantum dots. Nanoscale 12:4826–4832. https://doi.org/10.1039/C9NR10958G
46. Zaib M, Akhtar A, Maqsood F, Shahzadi T (2021) Green synthesis of carbon dots and their application as photocatalyst in dye degradation studies. Arab J Sci Eng 46:437–446
47. Kathiravan A, Gowri A, Srinivasan V, Smith TA, Ashokkumar M, Jhonsi MA (2020) A simple and ubiquitous device for picric acid detection in latent fingerprints using carbon dots. Analyst 145:4532–4539
48. Simiyon GG, Vergheese Thomas M, Nivetha B, and Parakkal MJ (2024) AI-authenticated latent fingerprint developed using ultra-bright nitrogen-doped carbon dots-intercalated Zn(OH)2 nanosheets. Chem Pap 78(10):6179–6189. https://doi.org/10.1007/s11696-024-03535-x.
49. Shawninder C, Macairan J-R, Yousefi N, Tufenkji N, Naccache R (2021) Green synthesis of carbon dots and their applications. J RSC Adv 11:25354–25363
50. Sheila Baker N and Baker GA (2010) Luminescent carbon nanodots: emergent nanolights. J Ger Chem Soc 49(38):6726–6744.https://doi.org/10.1002/anie.200906623.
51. Sharma V, Tiwari P, and Mobin SM (2017) Sustainable carbon-dots: recent advances in green carbon dots for sensing and bioimaging. J Mater Chem B 5:8904–8924
52. Park Y, Kim Y, Chang H, Won S, Kim H, Kwon W (2020) Biocompatible nitrogen-doped carbon dots: synthesis, characterization, and application. J Mater Chem B 8:8935–8951
53. Sharma A and Das J (2019) Small molecules derived carbon dots: synthesis and applications in sensing, catalysis, imaging, and biomedicine. J NanoBiotechnol 17(92)
54. Yoo D, Park Y, Cheon B, and Park MH (2019) Carbon dots as an effective fluorescent sensing platform for metal ion detection. Nanoscale Res Lett14:272
55. Aagesen DL (1998) Indigenous resource rights and conservation of the monkey-puzzle tree (Araucaria araucana, araucariaceae): a case study from Southern Chile. Econ Bot 52(2):146. https://doi.org/10.1007/BF02861203
56. Khan AW et al (2022) Potential biomedical applications of Araucaria araucana as an antispasmodic, bronchodilator, vasodilator, and antiemetic: involvement of calcium channels. J Ethnopharmacol 298. https://doi.org/10.1016/j.jep.2022.115651
57. Boehme SC, Vanmaekelbergh D, Evers WH, Siebbeles LDA, Houtepen AJ (2016) In situ spectroelectrochemical determination of energy levels and energy level offsets in quantum-dot heterojunctions. J Phys Chem C 120(9):5164–5173
58. Hsu P-C, Shih Z-Y, Lee C-H, Chang H-T (2012) Synthesis and analytical applications of photoluminescent carbon nanodots. Green Chem 14:917–920
59. Desai ML, Jha S, Basu H, Singhal RK, Par T-J, Kailasa SK (2019) Acid oxidation of muskmelon fruit for the fabrication of carbon dots with specific emission colors for recognition of Hg2+ ions and cell imaging. ACS Omega 4(21):19332–19340
60. Schmeda-Hirschmann G, Astudillo L, Rodríguez J, Theoduloz C, Yáñez T (2005) Gastroprotective effect of the mapuche crude drug Araucaria araucana resin and its main constituents. J Ethnopharmacol 101(1–3):271–276
61. Schmeda-Hirschmanna G, Astudillo L (2005) Gastroprotective effect and cytotoxicity of natural and semisynthetic labdane diterpenes from araucaria araucana resin. Z Für Naturforschung C 60(7–8):511–522
62. Abdelhamid HN, El-Bery HM, Metwally AA, Elshazly M, Hathout RM (2019) Synthesis of CdS-modified chitosan quantum dots for the drug delivery of Sesamol. Carbohydr Polym 214:90–99
63. Abdelhamid HN, Wu H-F (2013) Probing the interactions of chitosan capped CdS quantum dots with pathogenic bacteria and their biosensing application. J Mater Chem B 1:6094–6106
64. Bhaisare ML, Talib A, Khan MS, Pandey S, Wu H-F (2015) Synthesis of fluorescent carbon dots via microwave carbonization of citric acid in presence of tetraoctylammonium ion, and their application to cellular bioimaging. Microchim Acta 182:2173–2181
65. Briscoe J, Marinovic A, Sevilla M, Dunn S, and Titirici M (2015) Biomass-derived carbon quantum dot sensitizers for solid-state nanostructured solar cells. J Ger Chem Soc 54(15) :4463–4468
66. Liu J, Li R, Yang B (2020) Carbon dots: a new type of carbon-based nanomaterial with wide applications. ACS Cent Sci 6(12):2179–2195. https://doi.org/10.1021/acscentsci.0c01306
67. Hassan AQ, Barzani RK, Omer KM, Al-Hashimi BR, Mohammadi S, Salimi A (2021) Dual-emitter polymer carbon dots with spectral selection towards nanomolar detection of iron and aluminum ions. Arab J Chem 14(12). https://doi.org/10.1016/j.arabjc.2021.103452

68. Qiu H, Yuan F, Wang Y, Zhang Z, Li J, Li Y (2022) Green-light-emitting carbon dots *via* eco-friendly route and their potential in ferric-ion detection and WLEDs. Mater Adv 3(19):7339–7347. https://doi.org/10.1039/D2MA00520D
69. Bag P et al (2021) Recent development in synthesis of carbon dots from natural resources and their applications in biomedicine and multi-sensing platform. ChemistrySelect 6(11):2774–2789. https://doi.org/10.1002/slct.202100468
70. Bhamore JR, Jha S, Park TJ, Kailasa SK (2019) Green synthesis of multi-color emissive carbon dots from Manilkara zapota fruits for bioimaging of bacterial and fungal cells. J Photochem Photobiol B 191:150–155. https://doi.org/10.1016/j.jphotobiol.2018.12.023
71. Kanwal A et al (2022) Recent advances in green carbon dots (2015–2022): synthesis, metal ion sensing, and biological applications. Beilstein J Nanotechnol 13:1068–1107. https://doi.org/10.3762/bjnano.13.93
72. Goryacheva IYu, Sapelkin AV, Sukhorukov GB (2017) Carbon nanodots: Mechanisms of photoluminescence and principles of application. TrAC Trends Anal Chem 90:27–37. https://doi.org/10.1016/j.trac.2017.02.012
73. Atchudan R, Immanuel Edison TNJ, Perumal S, Sagaya Selvam NC, and Rok Lee Y (2019) Green synthesized multiple fluorescent nitrogen-doped carbon quantum dots as an efficient label-free optical nanoprobe for in vivo live-cell imaging. J Photochem Photobiol Chem 372:99–107
74. Yu Z, Zhang L, Wang X, He D, Suo H, Zhao C (2020) Fabrication of ZnO/carbon quantum dots composite sensor for detecting NO gas. Sens Basel 17:4961
75. Pal A, Bhakat A, Chattopadhyay A (2019) Zinc ion induced assembly of crystalline carbon dots with excellent supercapacitor performance. J Phys Chem C 123(32):19421–19428
76. Campanale C, Savino I, Massarelli C, Uricchio VF (2023) Fourier transform infrared spectroscopy to assess the degree of alteration of artificially aged and environmentally weathered microplastics. Polymers 15(4):911. https://doi.org/10.3390/polym15040911
77. Roy P, Chen P-C, Periasamy AP, Chen Y-N, Chang H-T (2015) Photoluminescent carbon nanodots: synthesis, physicochemical properties and analytical applications. Mater Today 18(8):447–458
78. Wang Y, Zhou S, Pan S, Sun X, Zhou J, and Li H (2023) Color-tunable carbon dots with aggregation-induced emission constructed by FRET between surface luminescence centers. Adv Opt Mater 2301486
79. Miao S, Liang K, Kong B (2020) Förster resonance energy transfer (FRET) paired carbon dot-based complex nanoprobes: versatile platforms for sensing and imaging applications. Mater Chem Front 4(1):128–139. https://doi.org/10.1039/C9QM00538B
80. Das S, Sarkar S, Das A (2021) A comprehensive review of various categories of face masks resistant to Covid-19. CEGH Home 12
81. Jung S, Lee S, Dou X, Kwon EE (2021) Valorization of disposable COVID-19 mask through the thermo-chemical process. Chem Eng J 405
82. De-la-Torre GE (2022) Release of phthalate esters (PAEs) and microplastics (MPs) from face masks and gloves during the COVID-19 pandemic. Environ Res 215(2). https://doi.org/10.1016/j.envres.2022.114337
83. Zuri G, Oró-Nolla B (2022) Migration of microplastics and phthalates from face masks to water. Molecules 27(20):6859
84. Ma J et al (2021) Face masks as a source of nanoplastics and microplastics in the environment: quantification, characterization, and potential for bioaccumulation. Environ Pollut 288. https://doi.org/10.1016/j.envpol.2021.117748
85. Morgana S, Casentini B, Amalfitano S (2021) Uncovering the release of micro/nanoplastics from disposable face masks at times of COVID-19. J Hazard Mater 419. https://doi.org/10.1016/j.jhazmat.2021.126507
86. Zhang J et al (2022) Effects of plastic residues and microplastics on soil ecosystems: a global meta-analysis. J Hazard Mater 435:129065. https://doi.org/10.1016/j.jhazmat.2022.129065
87. Tang Y, Zhang S, Su Y, Wu D, Zhao Y, Xie B (2021) Removal of microplastics from aqueous solutions by magnetic carbon nanotubes. Chem Eng J 406. https://doi.org/10.1016/j.cej.2020.126804
88. Tammina SK, Khan A, Rhim J-W (2023) Advances and prospects of carbon dots for microplastic analysis. Chemosphere 313. https://doi.org/10.1016/j.chemosphere.2022.137433